applied biosciences

MDPI

Communication

Phage Anti-Pycsar Proteins Efficiently Degrade β-Lactam Antibiotics

Pallav Joshi [1,2,†], Stefan Krco [1,2,†], Samuel J. Davis [1,2], Lachlan Asser [1], Thomas Brück [3], Rochelle M. Soo [1,2], Mikael Bodén [1], Philip Hugenholtz [1,2], Liam A. Wilson [4], Gerhard Schenk [1,5,*] and Marc T. Morris [1,2,*]

1 School of Chemistry and Molecular Biosciences, The University of Queensland, Brisbane, QLD 4072, Australia
2 Australian Centre for Ecogenomics, The University of Queensland, Brisbane, QLD 4072, Australia
3 Werner Siemens-Chair of Synthetic Biotechnology, TUM School of Natural Sciences, Technical University of Munich (TUM), 85748 Garching, Germany
4 Chemistry Research Laboratory, Department of Chemistry and the Ineos Oxford Institute for Antimicrobial Research, Oxford University, Oxford OX1 3TA, UK
5 Australian Institute of Bioengineering and Nanotechnology, The University of Queensland, Brisbane, QLD 4072, Australia
* Correspondence: schenk@uq.edu.au (G.S.); marc.morris@uq.edu.au (M.T.M.)
† These authors contributed equally to this work and share first authorship.

Abstract: Metallo-β-lactamases (MBLs) are members of the structurally conserved but functionally diverse MBL-fold superfamily of metallohydrolases. MBLs are a major concern for global health care as they efficiently inactivate β-lactam antibiotics, including the "last-resort" carbapenems, and no clinically suitable inhibitors are currently available. Increasingly, promiscuous β-lactamase activity is also observed in other members of the superfamily, including from viruses, which represents an underexplored reservoir for future pathways to antibiotic resistance. Here, two such MBL-fold enzymes from *Bacillus* phages, the cyclic mononucleotide-degrading proteins $Apyc_{Goe3}$ and $Apyc_{Grass}$, are shown to degrade β-lactam substrates efficiently *in vitro*. In particular, $Apyc_{Grass}$ displays a distinct preference for carbapenem substrates with a catalytic efficiency that is within one order of magnitude of the clinically relevant MBL NDM-1. Mutagenesis experiments also demonstrate that the loss of a metal-bridging aspartate residue reduces nuclease activity up to 35-fold but improves carbapenemase activity. In addition, we hypothesise that the oligomeric state significantly influences β-lactamase activity by modifying access to the active site pocket. Together, these observations hint at a possible new avenue of resistance via the spread of phage-borne MBL-fold enzymes with β-lactamase activity.

Keywords: virus; metallo-beta-lactamase (MBL); MBL-fold superfamily; antimicrobial resistance; anti-Pycsar; carbapanemase

Citation: Joshi, P.; Krco, S.; Davis, S.J.; Asser, L.; Brück, T.; Soo, R.M.; Bodén, M.; Hugenholtz, P.; Wilson, L.A.; Schenk, G.; et al. Phage Anti-Pycsar Proteins Efficiently Degrade β-Lactam Antibiotics. *Appl. Biosci.* **2024**, *3*, 438–449. https://doi.org/10.3390/applbiosci3040028

Academic Editor: Francesco Cappello

Received: 11 July 2024
Revised: 21 September 2024
Accepted: 8 October 2024
Published: 11 October 2024

1. Introduction

Antibiotic resistance has long been recognised as a critical global health concern [1]. The excessive use of antibiotics as preventive and curative measures against infection not only for human health but also in intensive animal husbandry has resulted in a widespread rise in antimicrobial resistance [2]. Amongst the varied mechanisms of antibiotic resistance, the production of β-lactamases, enzymes that break down β-lactam antibiotics, is of particular concern as they are the most widely used (~65% globally) and include "last-resort" antibiotics such as carbapenems (Figure 1A) [1,3]. These β-lactamases are classified based on their structure and mechanism as serine-β-lactamases (SBLs—Ambler classes A, C, and D; see Bush [4]), which utilise a conserved serine residue to hydrolyse the four-membered β-lactam ring, and metallo-β-lactamases (MBLs—Ambler class B), which catalyse the same reaction using a catalytic hydroxide coordinated by one or two zinc ions [3,5]. MBLs are of particular interest as no clinically useful inhibitors are currently available [3,5–7].

In contrast, SBLs are targeted by several potent and widely used drugs (e.g., clavulanic acid) [3,8,9].

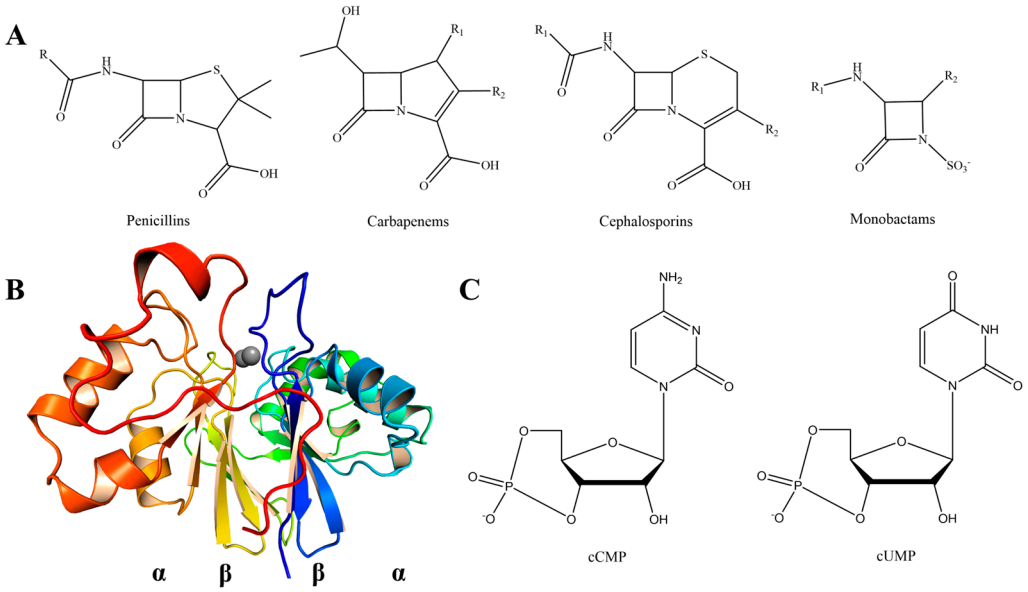

Figure 1. (**A**) Chemical structure of the backbones of the four major β-lactam antibiotic classes. (**B**) Overall structure of $Apyc_{Goe3}$ highlighting the αββα fold. The colouring is a gradient from blue (N-terminal) to red (C-terminal). The two grey spheres represent Zn(II) ions. The structural model was predicted using AlphaFold3 [10]. (**C**) Chemical structures of the following cyclic nucleotides: cyclic cytidine monophosphate (cCMP) and cyclic uridine monophosphate (cUMP).

MBLs are divided into the B1, B2, and B3 subgroups according to their phylogeny, active site residues, metal content, and substrate preferences [3,11,12]. The B1 and B2 subgroups contain the majority of the MBLs of current clinical concern [13], whereas B3 MBLs are primarily associated with environmental microorganisms [11,12,14,15], although some notable B3 members of concern (e.g., AIM-1) have been encountered in clinical environments [16,17]. The three subgroups belong to the MBL-fold protein superfamily [3,11], named after the first enzyme that was shown to contain the characteristic αββα or "MBL"-fold (Figure 1B), the MBL from *Bacillus cereus* (BcII) [18]. The MBL-fold superfamily is present in all domains of life, and while functionally diverse, they predominantly function as hydrolases. The members include, but are not limited to, endo- and exoribonucleases [19–21], phosphatases [22–24], lactonases [25,26], glyoxalases [27–29], dehalogenases [30], sulfatases [31,32], oxidases [33], and β-lactamases [11,12,34–38]. Recent studies have shown that numerous members of this superfamily exhibit catalytic promiscuity [39–43]. Promiscuous β-lactamase activity is of concern as the corresponding enzymes may represent a cryptic reservoir of antibiotic resistance. For example, two MBL-fold enzymes recovered from deep-sea viral metagenomes, i.e., TupBlac and PNGM-1, are nucleases with promiscuous β-lactamase activity [41,44,45]. While these native nucleases were likely acquired from a bacterial host, and their β-lactamase activity is currently marginal, their presence in a virus raises the question about the possible evolution and dissemination of antimicrobial resistance through horizontal gene transfer back into bacterial hosts.

During a sequence-based survey of B3 MBLs [12], we discovered two distantly related viral MBL-fold enzymes in the genomes of the *Bacillus* phage vB_Bsum_Goe3 (KY368640) and Grass virus (KF669652), which both belong to the "Bastille-like" viruses within the *Spounavirinae* subfamily of the *Myoviridae* [46,47] (note that phages are viruses that infect bacterial cells and coerce them to make more phages rather than cells [48]). These virally-encoded MBL-fold enzymes appear to have been horizontally-acquired from their bacterial hosts, but no closely-related characterised MBL-fold homologs were reported at that time. The recent characterisation of anti-Pycsar enzymes [49] sheds light on the likely

in vivo function of these enzymes. The Pyrimidine Cyclase System for Antiphage Resistance (Pycsar) is a recently identified but seemingly widespread bacterial defence mechanism against phages, which is activated by cyclic nucleotide messengers (Figure 1C) [50,51]. In response, *Bacillus* phages have evolved an anti-Pycsar system by expressing MBL-fold proteins that specifically cleave and thus inactivate cyclic nucleotide messengers [49]. One such anti-Pycsar protein, Apyc1 from the *Bacillus* phage Bsp38, shares 78.9% and 88.2% sequence identity with the vB_Bsum_Goe3 and Grass virus MBL-fold enzymes [49]. Therefore, we predicted that these MBL proteins should possess nuclease activity (i.e., $Apyc_{Goe3}$ and $Apyc_{Grass}$, respectively). However, since virally encoded β-lactamase activity has been demonstrated in TupBlac and PNGM-1, we evaluated the potential of both enzymatic properties in $Apyc_{Goe3}$ and $Apyc_{Grass}$. We recombinantly expressed the enzymes in an *Escherichia coli* host, followed by affinity chromatography purification via either an N-terminal maltose binding protein (MBP) or hexahistidine tag. (Note that both systems resulted in the production of soluble, pure enzymes. However, preliminary assays indicated that only the MBP-tagged enzymes displayed significant β-lactamase activity and hence were used for more detailed catalytic characterisation. Any attempts to remove the MBP tag by proteolytic cleavage resulted in the precipitation of the viral MBL proteins. Unless otherwise specified, the terms ApycGoe3 and ApycGrass correspond to the MBP-tagged constructs.) To assess their likely nucleolytic function, the RNase activity of these enzymes was quantitatively assessed using a fluorescence-based activity assay kit (RNase QC Alert kit, Thermo Fisher, Waltham, MA, USA) [44]. To test their β-lactamase activity, we performed continuous *in vitro* UV-Vis assays following the hydrolysis of representative β-lactam antibiotics.

2. Materials and Methods

The genes for $Apyc_{Goe3}$ (A0A217ER65) and $Apyc_{Grass}$ (U5PU04), as well as $Apyc_{Goe3}$ (D178S) and $Apyc_{Grass}$ (D161S), were cloned into both pMAL-c5x and pET-24a(+) vectors for subsequent tag-based affinity purification using either Maltose Binding Protein (MBP) or polyhistidine (6xHis) tags, respectively. The expression vectors containing the relevant genes were synthesised commercially (pMAL-c5x: Gene Universal Inc., Newark, DE, USA; pET-24a(+); Twist Biosciences, San Francisco, CA, USA).

The vectors were transferred into chemically competent *E. coli* Rosetta (DE3) cells via heat shock at 42 °C. Single, isolated colonies were picked and grown in LB medium supplemented with 100 μg/mL of either ampicillin (pMAL-c5x vectors) or kanamycin (pET-24a(+) vectors) for selection. These cultures were used to inoculate larger expression cultures of the LB medium with appropriate antibiotics and were grown under shaking (200 rpm) at 37 °C until they reached an $OD_{600} \approx 0.6$. At this point, protein expression was induced by adding 500 μM IPTG, reducing the temperature to 18 °C, and leaving the culture to grow for a further 12 h. The cells were harvested by centrifugation (20 min, 5000× *g*), resuspended in lysis buffer (20 mM Tris buffer, pH 8.0, containing 0.15 M NaCl, 150 μM $ZnCl_2$) supplemented with 1 mg/mL lysozyme, 1 mg/mL DNase I, and 1.5 mg/mL EDTA-free protease inhibitor cocktail, and lysed on ice by sonication. Cell debris was removed by centrifugation (40 min, 14,000× *g*), and the supernatant was loaded onto a 5 mL MBPTrap HP or HisTrap FF column for MBP- and polyhistidine-tagged enzymes, respectively, pre-equilibrated with purification buffer (20 mM Tris buffer, pH 8.0, containing 0.15 M NaCl, 150 μM $ZnCl_2$). The proteins were eluted against 10 mM maltose (MBPTrap HP) or 500 mM imidazole (HisTrap FF). Fractions containing the enzyme (determined by SDS-PAGE analysis; Supplementary Figures S1–S6) were pooled, and excess NaCl was removed via buffer exchange using EconoPac 10DG desalting columns (Bio-Rad, South Granville, NSW, Australia). For the polyhistidine-tagged $Apyc_{Goe3}$ and $Apyc_{Grass}$, the proteins were further purified via size exclusion chromatography by concentrating the proteins and then loading them onto a Hiprep 16/60 Sephacryl S-300 HR column (Cytiva, Marlborough, MA, USA) pre-equilibrated with purification buffer (20 mM Tris, pH 8.0). Both the polyhistidine- and MBP-tagged proteins were stored at 4 °C in 20 mM Tris buffer (pH 8.0).

To quantify hydrolytic activity towards nucleic acids, the activity of the two viral enzymes and two mutant enzymes was assessed against a mixed RNA substrate supplied by a commercially available nuclease activity kit (RNase QC Alert, Thermo Fisher, Waltham, MA, USA), which had been previously used to assess the nuclease activity of TupBlac [44]. The substrate is composed of ribonucleic acids with both a fluorescent probe and a quencher. Upon hydrolysis of the substrate, the fluorescent probe is no longer quenched, which allows for quantitative analysis of the amount of substrate hydrolysed. The assays were conducted in Costar 96-well flat bottom plates with final volumes of 200 µL at 37 °C for 1 h using a Clariostar TRF plate reader instrument (BMG Labtech, Victoria, Australia) at 490/520 nm excitation/emission via the time-resolved fluorescence function and analysed using Reader Control and MARS Data Analysis Software (V6.2, BMG Labtech, Victoria, Australia). Enzyme concentrations of 50 nM were used for all four tested enzymes. The nucleolytic activity of each enzyme was determined by comparison to a standard curve generated with RNase A. The standard curve was produced with 5, 10, 25, and 50 pg of RNase A. Assays were conducted in three independent experiments (triplicates).

The β-lactamase activity of the wild-type and serine mutant enzymes was tested by continuous *in vitro* UV-Vis assays against the following representative substrates from each major class of β-lactam antibiotics: ampicillin (λ = 235 nm; ε = 900 M^{-1} cm^{-1}), carbenicillin (λ = 235 nm; ε= 1190 M^{-1} cm^{-1}), penicillin G (λ = 235 nm; ε = 936 M^{-1} cm^{-1}), biapenem (λ = 293 nm; ε = 8630 M^{-1} cm^{-1}), imipenem (λ = 295 nm; ε = 9000 M^{-1} cm^{-1}), meropenem (λ = 297 nm; ε = 6500 M^{-1} cm^{-1}), cefaclor (λ = 280 nm; ε = 6410 M^{-1} cm^{-1}), cefuroxime (λ = 260 nm; ε = 9320 M^{-1} cm^{-1}), cephalothin (λ = 265 nm; ε = 8790 M^{-1} cm^{-1}), and aztreonam (λ = 318 nm; ε = 660 M^{-1} cm^{-1}). The assays were run for 1 min at 25 °C in 50 mM Tris (pH 8.0) using enzyme concentrations of 0.5 µM for $Apyc_{Goe3}$, $Apyc_{Goe3}$ (D178S), and $Apyc_{Grass}$ and 0.3–0.5 µM for $Apyc_{Grass}$ (D161S). The data were measured in triplicates, and the Michaelis–Meten parameters were determined by nonlinear fitting using Graphpad Prism 9 (Figure S7). All β-lactamase assays were run on an Agilent Cary 60 UV-Vis Spectrophotometer (Santa Clara, CA, USA).

3. Results and Discussion

As predicted, $Apyc_{Goe3}$ and $Apyc_{Grass}$ possess significant RNAse activity (see Figure 2 and the details below), supporting the designation of these enzymes as orthologs of Apyc1. Concerningly, $Apyc_{Goe3}$ and $Apyc_{Grass}$ also display significant levels of β-lactamase activity (Table 1). For $Apyc_{Grass}$, the catalytic efficiencies (k_{cat}/K_M) are greatest for carbapenem substrates (10–15 s^{-1} mM^{-1}), followed by penicillins (0.5–3 s^{-1} mM^{-1}), while cephalosporins are less readily hydrolysed (≥0.1 s^{-1} mM^{-1}). The preference for carbapenems is due to both higher catalytic rates and lower K_M values when compared with penicillins. Interestingly, cephalosporins bind more strongly to $Apyc_{Grass}$ than the other substrates but are turned over extremely slowly. For $Apyc_{Goe3}$, the catalytic efficiencies are similar for carbapenems (~1 s^{-1} mM^{-1}) and penicillins (1–3 s^{-1} mM^{-1}) and are approximately two- to ten-fold higher than for cephalosporins (0.1–0.5 s^{-1} mM^{-1}). Similar to $Apyc_{Grass}$, the cephalosporins bind significantly tighter than the other substrates but are turned over very slowly. This suggests that while cephalosporins can bind tightly, they are likely oriented in a catalytically non-competent conformation. Consistent with this interpretation is the observation that cephalosporins, but not the other major classes of β-lactams, are competitive inhibitors of other MBL-fold enzymes, namely, SNM1A and SNM1B, two human MBL-fold enzymes involved in DNA repair, with IC50 values in the low µM range [52]. These results suggest that non-competent binding of cephalosporins or inhibitory effects of these β-lactams may be a more common characteristic across the MBL-fold superfamily than previously appreciated and hence warrants further investigation.

Table 1. Catalytic parameters of the MBP-tagged wild-type and mutant forms of the virally encoded $Apyc_{Goe3}$ and $Apyc_{Grass}$ recorded with representative substrates from all major classes of β-lactam antibiotics. Units of k_{cat}, K_M, and k_{cat}/K_M are s^{-1}, μM, and s^{-1} mM^{-1} | N.H.—no hydrolytic activity detected. [a] Lee et al. [53]. Errors are shown as standard errors from the mean using triplicate measurements.

	$Apyc_{Goe3}$			$Apyc_{Goe3}$ (D178S)			$Apyc_{Grass}$			$Apyc_{Grass}$ (D161S)			PNGM-1 [a]		
Substrate	k_{cat}	K_M	k_{cat}/K_M	k_{cat}	K_M	k_{cat}/K_M	k_{cat}	K_M	k_{cat}/K_M	k_{cat}	K_M	k_{cat}/K_M	k_{cat}	K_M	k_{cat}/K_M
Penicillins															
Penicillin G	$0.24 \pm 4 \times 10^{-2}$	230 ± 47	1.04	$0.45 \pm 5 \times 10^{-2}$	751 ± 158	0.60	$0.67 \pm 6 \times 10^{-2}$	231 ± 55	2.90	$0.48 \pm 3 \times 10^{-2}$	180 ± 35	2.70	7.5×10^{-2}	16	4.7
Ampicillin	1.8 ± 0.1	663 ± 94	2.67	$0.72 \pm 7 \times 10^{-2}$	526 ± 91	1.37	$0.54 \pm 7 \times 10^{-2}$	418 ± 102	1.29	$0.39 \pm 5 \times 10^{-2}$	891 ± 177	0.44	2.7×10^{-2}	15	1.8
Carbenicillin	$0.32 \pm 2 \times 10^{-2}$	205 ± 39	1.56	$0.13 \pm 9 \times 10^{-3}$	157 ± 29	0.83	$0.15 \pm 2 \times 10^{-2}$	330 ± 82	0.45	$0.24 \pm 4 \times 10^{-2}$	462 ± 148	0.52	-	-	-
Carbapenems															
Meropenem	$0.22 \pm 2 \times 10^{-2}$	215 ± 57	1.02	$0.43 \pm 4 \times 10^{-2}$	160 ± 32	2.69	$1.1 \pm 9 \times 10^{-2}$	98 ± 26	11.2	4.4 ± 0.7	287 ± 83	15.3	8.0×10^{-4}	2	0.42
Imipenem	$0.27 \pm 3 \times 10^{-2}$	436 ± 33	0.62	-	-	-	3.1 ± 0.42	200 ± 54	15.5	4.2 ± 0.6	253 ± 56	16.6	1.1×10^{-3}	2	0.55
Cephalosporins															
Cefuroxime	$8.6 \times 10^{-3} \pm 4 \times 10^{-4}$	18 ± 3	0.48	$8.3 \times 10^{-3} \pm 3 \times 10^{-4}$	3.5 ± 0.5	2.37	$5.3 \times 10^{-3} \pm 2 \times 10^{-4}$	44 ± 9	0.12	$6.0 \times 10^{-3} \pm 9 \times 10^{-4}$	142 ± 43	0.042	-	-	-
Cephalothin	$3.0 \times 10^{-3} \pm 2 \times 10^{-4}$	19 ± 6	0.16	$7.0 \times 10^{-3} \pm 5 \times 10^{-4}$	23 ± 4	0.30	$5.6 \times 10^{-3} \pm 4 \times 10^{-4}$	51 ± 11	0.11	$1.3 \times 10^{-3} \pm 1 \times 10^{-4}$	54 ± 18	0.024	0.13	62	2.1
Monobactams															
Aztreonam	N.H.	N.H.	N.H.	N.H.	N.H.	N.H.	N.H.	N.H.	N.H.	N.H.	N.H.	N.H.	-	-	-

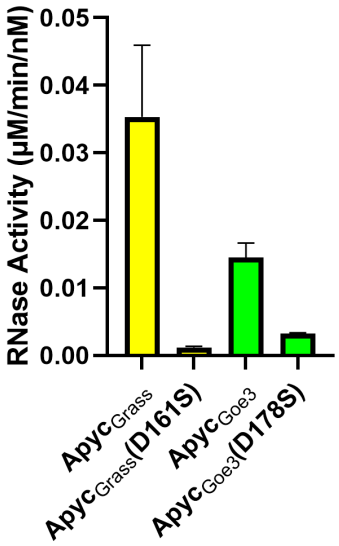

Figure 2. Nuclease activity of Apyc$_{Grass}$, Apyc$_{Grass}$ (D161S), Apyc$_{Goe3}$, and Apyc$_{Goe3}$ (D178S) using a mixed ribonucleic acid substrate tagged with a fluorescent probe from the RNase QC Alert kit (Thermo Fisher, Waltham, MA, USA). Activity was obtained by comparison to a standard curve generated with an RNase A positive control.

It should be noted that Apyc$_{Goe3}$ and Apyc$_{Grass}$ are significantly more efficient as β-lactamases than other virally encoded enzymes from the MBL-fold superfamily. For comparison, PNGM-1 has k_{cat}/K_M ratios comparable to those of Apyc$_{Goe3}$ and Apyc$_{Grass}$ for penicillins and carbapenems (~0.5–5 s^{-1} mM^{-1}); however, they all appear to bind in catalytically non-competent conformations (leading to k_{cat} values of 10^{-2}–10^{-4} s^{-1}; Table 1). In particular, the carbapenemase activity of Apyc$_{Grass}$ (k_{cat} ~ 1–3 s^{-1}; k_{cat}/K_M ~ 10–15 s^{-1} mM^{-1}) is remarkable, even when compared with "true" MBLs such as the B1 MBL NDM-1, an enzyme that is recognised as a globally distributed clinical concern [1,54] (Table S1). The k_{cat} and k_{cat}/K_M values of the NDM-1-catalysed hydrolysis of the carbapenems meropenem (12 s^{-1}, 250 s^{-1} mM^{-1}) and imipenem (20 s^{-1}, 210 s^{-1} mM^{-1}) are only one order of magnitude greater than those of Apyc$_{Grass}$. Furthermore, we also note that the turnover rates of both Apyc$_{Goe3}$ and Apyc$_{Grass}$ are comparable and, in some cases, superior to those of some SBLs such as the clinically relevant AmpC and OXA-48 (Table S1). This may indicate that these enzymes are predisposed to further evolve into efficient carbapenemases, which could constitute a threat to current treatment options for infections.

Sequence alignments and AlphaFold3 models suggest that both Apyc$_{Goe3}$ and Apyc$_{Grass}$ contain the canonical HHH/DHH metal-binding motif observed in B3 MBLs and across the broader MBL-fold superfamily [3,11] (Figures 3 and S8). Notably, they possess the aspartate residue found in the majority of non-β-lactamase MBL-fold hydrolases, which bridges the two metal ions in the active site. This aspartate residue has been suggested to be critical to catalysis in several MBL-fold enzymes [39,55], but it is notably substituted by non-metal-coordinating residues in all true β-lactamase lineages of the superfamily (i.e., in the B1, B2, and B3 MBLs), potentially implying a key role for this residue in the evolution of β-lactamase activity. The replacement of this metal-bridging ligand in class B β-lactamases may facilitate greater structural flexibility (i.e., reduced rigidity), possibly a feature that is important to accommodate a large number of diverse β-lactam substrates. To test this hypothesis, mutant variants of Apyc$_{Goe3}$ and Apyc$_{Grass}$ were generated, in which this aspartate residue was replaced by a serine residue, as is found in B3 MBLs [11].

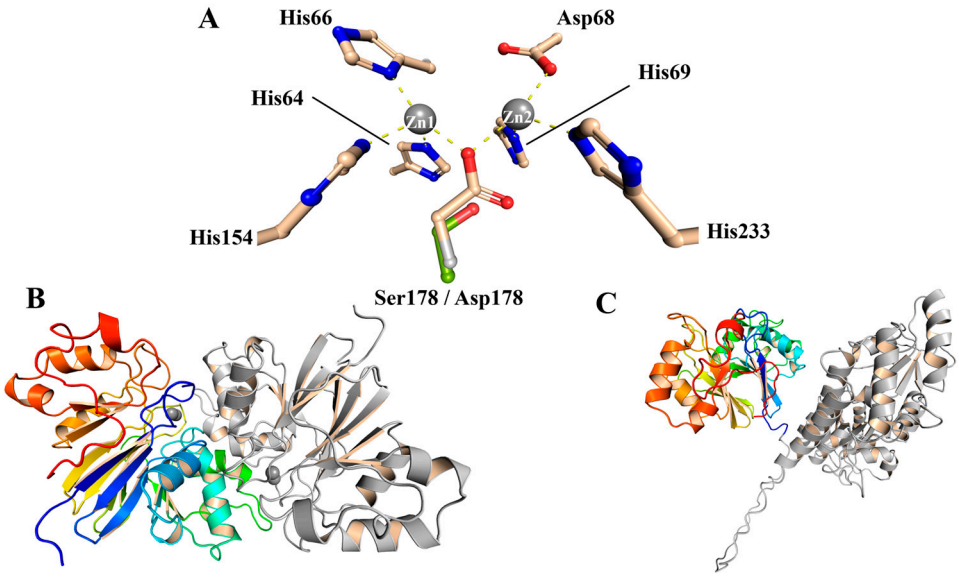

Figure 3. (**A**) Active site of $Apyc_{Goe3}$ showing the aspartate-to-serine mutation observed in $Apyc_{Goe3}$ (D178S), which removes a coordination point for each metal (Zn^{2+}) ion. (**B**) Overall structure of the polyhistidine-tagged $Apyc_{Goe3}$ dimer. One monomer is coloured in a gradient from blue (N-terminus) to red (C-terminus), and the other is coloured grey. (**C**) Overall structure of the MBP-tagged $Apyc_{Goe3}$ monomer. The $Apyc_{Goe3}$ portion of the fusion protein is coloured in a gradient from blue (N-terminus) to red (C-terminus), whereas the MBP tag is coloured grey. All structural models were predicted using AlphaFold 3 [10].

The mutation has, however, minimal impact on the catalytic properties using carbapenems and penicillins as substrates. The preference for carbapenems is retained with k_{cat}/K_M values of ~2 s^{-1} mM^{-1} and 15 s^{-1} mM^{-1} for $Apyc_{Goe3}$ and $Apyc_{Grass}$, respectively (Table 1). For the penicillin substrates, the corresponding values are 0.5–1.5 s^{-1} mM^{-1} and 0.5–3 s^{-1} mM^{-1}. The cephalosporins are again turned over very slowly, but because of the very low K_M values in $Apyc_{Goe3}$, they reach k_{cat}/K_M values similar to that of the other substrates. While the introduction of the aspartate to serine mutation had a modest impact on the β-lactamase activity of $Apyc_{Goe3}$ and $Apyc_{Grass}$, it reduced their nuclease activity by 5- and 35-fold, respectively. The RNase activity of the native forms of $Apyc_{Goe3}$ and $Apyc_{Grass}$ displayed nuclease activities of 4054 mU/min and 10,115 mU/min (equivalent to ~0.015 μM/min/nM and ~0.035 μM/min/nM; Figure 2), while the mutant enzymes displayed activities of 810 mU/min and 289 mU/min, respectively. In comparison, TupBlac, a dual-activity MBL-fold enzyme from a giant mimivirus, was reported to possess a nuclease activity of 0.451 mU/min [44]. It thus appears that both the native and mutant forms of $Apyc_{Goe3}$ and $Apyc_{Grass}$ readily degrade β-lactam antibiotics as well as ribonucleic acids and do so more efficiently than comparable viral MBL-fold nucleases, although nuclease activity is greatly diminished in the serine mutant enzymes. Hence, our study demonstrates that while the aspartate residue that is present in the active site of many MBL-fold superfamily members is important for nuclease activity, its contribution to β-lactamase activity is less significant. The loss of this aspartate residue may thus have been a mechanism to enable ancestral MBL-fold hydrolases to accelerate their evolution towards β-lactamase, but other as of yet unknown factors also contribute towards this functional transition.

Interestingly, the hexahistidine-tagged variants of both enzymes display nuclease but no β-lactamase activity (data not shown). A possible explanation for the observed discrepancy in the activity profiles of the different variants may be the impact of the tags on the oligomeric state of these enzymes. We hypothesise that because of its size, the MBP tag prevents the oligomerisation of $Apyc_{Goe3}$ and $Apyc_{Grass}$, while the histidine-tagged variants may form dimers or even higher oligomers. Indeed, structural prediction using AlphaFold3 suggested that the native and polyhistidine-tagged variants form dimers, whereas the

enzymes tagged with the larger MBP tag were monomeric (Figure 3). It is noteworthy that most of the highly active "true" MBLs (e.g., NDM-1, AIM-1) are monomeric, while many nucleases such as the RNase Zs are dimeric [19]. In addition, the crystal structure of PNGM-1 (PDB code: 6J4N) suggests that the protein may be tetrameric [45], while structural modelling of TupBlac reveals considerable structural similarity to the dimeric RNase Zs [44]. These results thus raise the possibility that both TupBlac and PNGM-1, as well as multimeric MBL-fold hydrolases more broadly, may be functionalised into more efficient β-lactamases by altering their oligomeric states to monomers, which may enhance the accessibility of the active site for β-lactam substrates.

4. Conclusions

The present study provides evidence that anti-Pycsar proteins from the MBL-fold superfamily are capable of efficient β-lactam hydrolysis, and notably display a preference for the "last-resort" carbapenems. However, their β-lactamase activity may be dependent on their oligomeric state. The metal-bridging aspartate residue present in the large majority of MBL-fold enzymes, but absent in "true" MBLs, appears to have minimal effect on β-lactamase activity (Table 1), but its removal greatly impairs nuclease activity (Figure 2). The evolution of "true" MBLs from an MBL-fold hydrolase precursor could thus have arisen from a concerted effect of structural changes that may alter the oligomeric state and the removal of a metal–ligand that leads to a change in the preferred substrate towards β-lactams. Given that phages can be vectors of horizontal transfer of genes between bacterial hosts, the possible evolution of an efficient β-lactamase from a phage-encoded MBL-fold nuclease, in particular, anti-Pycsar enzymes, could represent a new avenue for the rapid dissemination of antimicrobial resistance and thus pose a significant threat to human health. It is thus very important to gain insight into the environmental conditions (e.g., high bacterial density, stress conditions, presence of mobile genetic elements, nutrient availability) that facilitate or promote horizontal transfer of relevant genes as one avenue to stem the possible spread of antibiotic resistance. As the number of known enzymes within the MBL superfamily with cryptic β-lactamase activity grows, it will also become increasingly more important to design specific inhibition strategies to prevent this activity from providing novel avenues of antibiotic resistance. It is hoped that studies like the present one will stimulate a concerted, global effort in this quest.

Supplementary Materials: The following supporting information can be downloaded at https://www.mdpi.com/article/10.3390/applbiosci3040028/s1: Materials and Methods; Figures S1–S6: SDS-PAGE gels of purified protein samples, Figure S7: Representative Michaelis–Menten curves for reactions catalysed by $Apyc_{Goe3}$, $Apyc_{Goe3(D178S)}$, $Apyc_{Grass}$, and $Apyc_{Grass\ (D161S)}$ with relevant substrates. Figure S8: Alignment of metal-binding residues of Apyc orthologs and representatives of the MBL-fold superfamily; Table S1: Catalytic parameters of representative members of each Ambler class of β-lactamases. References [56–70] relate to the content in the Supplementary Materials.

Author Contributions: Conceptualisation, S.J.D., L.A.W., R.M.S., M.B., P.H., G.S. and M.T.M.; methodology, P.J., S.K., S.J.D., L.A.W. and M.T.M.; software—validation, T.B., R.M.S., M.B., P.H., G.S. and M.T.M.; formal analysis, P.J., S.K., S.J.D., L.A., L.A.W., and M.T.M.; investigation, P.J., S.K., L.A. and L.A.W.; resources, R.M.S., M.B., P.H., G.S. and M.T.M.; data curation, S.J.D. and L.A.W.; writing—original draft preparation, P.J., S.K., S.J.D. and M.T.M.; writing—review and editing, P.J., S.K., S.J.D., L.A., L.A.W., T.B., R.M.S., M.B., P.H., G.S. and M.T.M.; visualisation, S.J.D., S.K. and M.T.M.; supervision, T.B., R.M.S., M.B., P.H., G.S. and M.T.M.; project administration, P.H., G.S. and M.T.M.; funding acquisition, R.M.S., M.B., P.H. and G.S. All authors have read and agreed to the published version of the manuscript.

Funding: This research was funded by the National Health and Medical Research Council from Australia, Ideas Grant ID 2013090.

Institutional Review Board Statement: Not Applicable.

Informed Consent Statement: Not Applicable.

Data Availability Statement: The raw data supporting the conclusions of this article will be made available by the authors on request.

Conflicts of Interest: The authors declare no conflicts of interest. The funders had no role in the design of this study; in the collection, analyses, or interpretation of data; in the writing of this manuscript; or in the decision to publish the results.

References

1. World Health Organization. *Antimicrobial Resistance: Global Report on Surveillance*; World Health Organization: Geneva, Switzerland, 2014; ISBN 978-92-4-156474-8.
2. Mann, A.; Nehra, K.; Rana, J.S.; Dahiya, T. Antibiotic Resistance in Agriculture: Perspectives on Upcoming Strategies to Overcome Upsurge in Resistance. *Curr. Res. Microb. Sci.* **2021**, *2*, 100030. [CrossRef]
3. Bahr, G.; González, L.J.; Vila, A.J. Metallo-β-Lactamases in the Age of Multidrug Resistance: From Structure and Mechanism to Evolution, Dissemination, and Inhibitor Design. *Chem. Rev.* **2021**, *121*, 7957–8094. [CrossRef]
4. Bush, K. The ABCD's of β-Lactamase Nomenclature. *J. Infect. Chemother.* **2013**, *19*, 549–559. [CrossRef]
5. Brem, J.; Panduwawala, T.; Hansen, J.U.; Hewitt, J.; Liepins, E.; Donets, P.; Espina, L.; Farley, A.J.M.; Shubin, K.; Campillos, G.G.; et al. Imitation of β-Lactam Binding Enables Broad-Spectrum Metallo-β-Lactamase Inhibitors. *Nat. Chem.* **2022**, *14*, 15–24. [CrossRef]
6. Arjomandi, O.K.; Hussein, W.M.; Vella, P.; Yusof, Y.; Sidjabat, H.E.; Schenk, G.; McGeary, R.P. Design, Synthesis, and in Vitro and Biological Evaluation of Potent Amino Acid-Derived Thiol Inhibitors of the Metallo-β-Lactamase IMP-1. *Eur. J. Med. Chem.* **2016**, *114*, 318–327. [CrossRef]
7. McGeary, R.P.; Tan, D.T.C.; Selleck, C.; Monteiro Pedroso, M.; Sidjabat, H.E.; Schenk, G. Structure-Activity Relationship Study and Optimisation of 2-Aminopyrrole-1-Benzyl-4,5-Diphenyl-1H-Pyrrole-3-Carbonitrile as a Broad Spectrum Metallo-β-Lactamase Inhibitor. *Eur. J. Med. Chem.* **2017**, *137*, 351–364. [CrossRef]
8. Neu, H.C.; Fu, K.P. Clavulanic Acid, a Novel Inhibitor of β-Lactamases. *Antimicrob. Agents Chemother.* **1978**, *14*, 650–655. [CrossRef]
9. Tooke, C.L.; Hinchliffe, P.; Bragginton, E.C.; Colenso, C.K.; Hirvonen, V.H.A.; Takebayashi, Y.; Spencer, J. β-Lactamases and β-Lactamase Inhibitors in the 21st Century. *J. Mol. Biol.* **2019**, *431*, 3472–3500. [CrossRef]
10. Abramson, J.; Adler, J.; Dunger, J.; Evans, R.; Green, T.; Pritzel, A.; Ronneberger, O.; Willmore, L.; Ballard, A.J.; Bambrick, J.; et al. Accurate Structure Prediction of Biomolecular Interactions with AlphaFold 3. *Nature* **2024**, *630*, 493–500. [CrossRef]
11. Krco, S.; Davis, S.J.; Joshi, P.; Wilson, L.A.; Monteiro Pedroso, M.; Douw, A.; Schofield, C.J.; Hugenholtz, P.; Schenk, G.; Morris, M.T. Structure, Function, and Evolution of Metallo-β-Lactamases from the B3 Subgroup—Emerging Targets to Combat Antibiotic Resistance. *Front. Chem.* **2023**, *11*, 1196073. [CrossRef]
12. Pedroso, M.M.; Waite, D.W.; Melse, O.; Wilson, L.; Mitić, N.; McGeary, R.P.; Antes, I.; Guddat, L.W.; Hugenholtz, P.; Schenk, G. Broad Spectrum Antibiotic-Degrading Metallo-β-Lactamases Are Phylogenetically Diverse. *Protein Cell* **2020**, *11*, 613–617. [CrossRef]
13. Bush, K.; Bradford, P.A. β-Lactams and β-Lactamase Inhibitors: An Overview. *Cold Spring Harb. Perspect. Med.* **2016**, *6*, a025247. [CrossRef] [PubMed]
14. Pedroso, M.M.; Selleck, C.; Enculescu, C.; Harmer, J.R.; Mitić, N.; Craig, W.R.; Helweh, W.; Hugenholtz, P.; Tyson, G.W.; Tierney, D.L.; et al. Characterization of a Highly Efficient Antibiotic-Degrading Metallo-β-Lactamase Obtained from an Uncultured Member of a Permafrost Community. *Metallomics* **2017**, *9*, 1157–1168. [CrossRef]
15. Vella, P.; Miraula, M.; Phelan, E.; Leung, E.W.W.; Ely, F.; Ollis, D.L.; McGeary, R.P.; Schenk, G.; Mitić, N. Identification and Characterization of an Unusual Metallo-β-Lactamase from Serratia Proteamaculans. *JBIC J. Biol. Inorg. Chem.* **2013**, *18*, 855–863. [CrossRef]
16. Yong, D.; Toleman Mark, A.; Bell, J.; Ritchie, B.; Pratt, R.; Ryley, H.; Walsh Timothy, R. Genetic and Biochemical Characterization of an Acquired Subgroup B3 Metallo-β-Lactamase Gene, blaAIM-1, and Its Unique Genetic Context in *Pseudomonas aeruginosa* from Australia. *Antimicrob. Agents Chemother.* **2012**, *56*, 6154–6159. [CrossRef]
17. Zhou, H.; Guo, W.; Zhang, J.; Li, Y.; Zheng, P.; Zhang, H. Draft Genome Sequence of a Metallo-β-Lactamase (Bla(AIM-1))-Producing *Klebsiella pneumoniae* ST1916 Isolated from a Patient with Chronic Diarrhoea. *J. Glob. Antimicrob. Resist.* **2019**, *16*, 165–167. [CrossRef]
18. Carfi, A.; Pares, S.; Duée, E.; Galleni, M.; Duez, C.; Frère, J.M.; Dideberg, O. The 3-D Structure of a Zinc Metallo-Beta-Lactamase from Bacillus Cereus Reveals a New Type of Protein Fold. *EMBO J.* **1995**, *14*, 4914–4921. [CrossRef]
19. Dominski, Z. Nucleases of the Metallo-Beta-Lactamase Family and Their Role in DNA and RNA Metabolism. *Crit. Rev. Biochem. Mol. Biol.* **2007**, *42*, 67–93. [CrossRef]
20. Dominski, Z.; Carpousis, A.J.; Clouet-d'Orval, B. Emergence of the β-CASP Ribonucleases: Highly Conserved and Ubiquitous Metallo-Enzymes Involved in Messenger RNA Maturation and Degradation. *Biochim. Biophys. Acta BBA-Gene Regul. Mech.* **2013**, *1829*, 532–551. [CrossRef]
21. Pettinati, I.; Brem, J.; Lee, S.Y.; McHugh, P.J.; Schofield, C.J. The Chemical Biology of Human Metallo-β-Lactamase Fold Proteins. *Trends BioChem. Sci.* **2016**, *41*, 338–355. [CrossRef]

22. Beaudoin, G.A.W.; Li, Q.; Bruner, S.D.; Hanson, A.D. An Unusual Diphosphatase from the PhnP Family Cleaves Reactive FAD Photoproducts. *Biochem. J.* **2018**, *475*, 261–272. [CrossRef] [PubMed]
23. Castillo Villamizar Genis, A.; Funkner, K.; Nacke, H.; Foerster, K.; Daniel, R.; Sawers, G. Functional Metagenomics Reveals a New Catalytic Domain, the Metallo-β-Lactamase Superfamily Domain, Associated with Phytase Activity. *mSphere* **2019**, *4*, e00167-19. [CrossRef]
24. Ng, T.K.; Gahan, L.R.; Schenk, G.; Ollis, D.L. Altering the Substrate Specificity of Methyl Parathion Hydrolase with Directed Evolution. *Arch. BioChem. Biophys.* **2015**, *573*, 59–68. [CrossRef]
25. Fernandez, F.J.; Garces, F.; López-Estepa, M.; Aguilar, J.; Baldomà, L.; Coll, M.; Badia, J.; Vega, M.C. The UlaG Protein Family Defines Novel Structural and Functional Motifs Grafted on an Ancient RNase Fold. *BMC Evol. Biol.* **2011**, *11*, 273. [CrossRef]
26. Miraula, M.; Whitaker, J.J.; Schenk, G.; Mitić, N. β-Lactam Antibiotic-Degrading Enzymes from Non-Pathogenic Marine Organisms: A Potential Threat to Human Health. *J. Biol. Inorg. Chem.* **2015**, *20*, 639–651. [CrossRef]
27. Au, S.X.; Dzulkifly, N.S.; Muhd Noor, N.D.; Matsumura, H.; Raja Abdul Rahman, R.N.Z.; Normi, Y.M. Dual Activity BLEG-1 from *Bacillus lehensis* G1 Revealed Structural Resemblance to B3 Metallo-β-Lactamase and Glyoxalase II: An Insight into Its Enzyme Promiscuity and Evolutionary Divergence. *Int. J. Mol. Sci.* **2021**, *22*, 9377. [CrossRef] [PubMed]
28. Tan, S.H.; Normi, Y.M.; Leow, A.T.C.; Salleh, A.B.; Murad, A.M.A.; Mahadi, N.M.; Rahman, M.B.A. Danger Lurking in the "Unknowns": Structure-to-Function Studies of Hypothetical Protein Bleg1_2437 from *Bacillus lehensis* G1 Alkaliphile Revealed an Evolutionary Divergent B3 Metallo-Beta-Lactamase. *J. Biochem.* **2017**, *161*, 167–186. [CrossRef]
29. Vašková, J.; Kočan, L.; Vaško, L.; Perjési, P. Glutathione-Related Enzymes and Proteins: A Review. *Molecules* **2023**, *28*, 1447. [CrossRef]
30. Wang, G.; Li, R.; Li, S.; Jiang, J. A Novel Hydrolytic Dehalogenase for the Chlorinated Aromatic Compound Chlorothalonil. *J. Bacteriol.* **2010**, *192*, 2737–2745. [CrossRef]
31. Barbeyron, T.; Potin, P.; Richard, C.; Collin, O.; Kloareg, B. Arylsulphatase from *Alteromonas carrageenovora*. *Microbiology* **1995**, *141 Pt. 11*, 2897–2904. [CrossRef]
32. Hagelueken, G.; Adams Thorsten, M.; Wiehlmann, L.; Widow, U.; Kolmar, H.; Tümmler, B.; Heinz Dirk, W.; Schubert, W.-D. The Crystal Structure of SdsA1, an Alkylsulfatase from *Pseudomonas aeruginosa*, Defines a Third Class of Sulfatases. *Proc. Natl. Acad. Sci. USA* **2006**, *103*, 7631–7636. [CrossRef]
33. Muok, A.R.; Deng, Y.; Gumerov, V.M.; Chong, J.E.; DeRosa, J.R.; Kurniyati, K.; Coleman, R.E.; Lancaster, K.M.; Li, C.; Zhulin, I.B.; et al. A Di-Iron Protein Recruited as an Fe[II] and Oxygen Sensor for Bacterial Chemotaxis Functions by Stabilizing an Iron-Peroxy Species. *Proc. Natl. Acad. Sci. USA* **2019**, *116*, 14955–14960. [CrossRef]
34. Morán-Barrio, J.; Lisa, M.-N.; Larrieux, N.; Drusin, S.I.; Viale, A.M.; Moreno, D.M.; Buschiazzo, A.; Vila, A.J. Crystal Structure of the Metallo-β-Lactamase GOB in the Periplasmic Dizinc Form Reveals an Unusual Metal Site. *Antimicrob. Agents Chemother.* **2016**, *60*, 6013–6022. [CrossRef] [PubMed]
35. Selleck, C.; Larrabee, J.A.; Harmer, J.; Guddat, L.W.; Mitić, N.; Helweh, W.; Ollis, D.L.; Craig, W.R.; Tierney, D.L.; Monteiro Pedroso, M.; et al. AIM-1: An Antibiotic-Degrading Metallohydrolase That Displays Mechanistic Flexibility. *Chem.-Eur. J.* **2016**, *22*, 17704–17714. [CrossRef]
36. Wilson, L.A.; Knaven, E.G.; Morris, M.T.; Monteiro Pedroso, M.; Schofield, C.J.; Brück, T.B.; Boden, M.; Waite, D.W.; Hugenholtz, P.; Guddat, L.; et al. Kinetic and Structural Characterization of the First B3 Metallo-β-Lactamase with an Active-Site Glutamic Acid. *Antimicrob. Agents Chemother.* **2021**, *65*, e00936-21. [CrossRef]
37. Yong, D.; Toleman, M.A.; Giske, C.G.; Cho, H.S.; Sundman, K.; Lee, K.; Walsh, T.R. Characterization of a New Metallo-β-Lactamase Gene, blaNDM-1, and a Novel Erythromycin Esterase Gene Carried on a Unique Genetic Structure in *Klebsiella pneumoniae* Sequence Type 14 from India. *Antimicrob. Agents Chemother.* **2009**, *53*, 5046–5054. [CrossRef]
38. Garau, G.; Bebrone, C.; Anne, C.; Galleni, M.; Frère, J.-M.; Dideberg, O. A Metallo-β-Lactamase Enzyme in Action: Crystal Structures of the Monozinc Carbapenemase CphA and Its Complex with Biapenem. *J. Mol. Biol.* **2005**, *345*, 785–795. [CrossRef]
39. Diene, S.M.; Pinault, L.; Keshri, V.; Armstrong, N.; Khelaifia, S.; Chabrière, E.; Caetano-Anolles, G.; Colson, P.; La Scola, B.; Rolain, J.-M.; et al. Human Metallo-β-Lactamase Enzymes Degrade Penicillin. *Sci. Rep.* **2019**, *9*, 12173. [CrossRef]
40. Diene, S.M.; Pinault, L.; Armstrong, N.; Azza, S.; Keshri, V.; Khelaifia, S.; Chabrière, E.; Caetano-Anolles, G.; Rolain, J.-M.; Pontarotti, P.; et al. Dual RNase and β-Lactamase Activity of a Single Enzyme Encoded in Archaea. *Life* **2020**, *10*, 280. [CrossRef]
41. Lee, J.H.; Takahashi, M.; Jeon, J.H.; Kang, L.-W.; Seki, M.; Park, K.S.; Hong, M.-K.; Park, Y.S.; Kim, T.Y.; Karim, A.M.; et al. Dual Activity of PNGM-1 Pinpoints the Evolutionary Origin of Subclass B3 Metallo-β-Lactamases: A Molecular and Evolutionary Study. *Emerg. Microbes Infect.* **2019**, *8*, 1688–1700. [CrossRef]
42. Miraula, M.; Schenk, G.; Mitić, N. Promiscuous Metallo-β-Lactamases: MIM-1 and MIM-2 May Play an Essential Role in Quorum Sensing Networks. *J. Inorg. Biochem.* **2016**, *162*, 366–375. [CrossRef] [PubMed]
43. Perez-Garcia, P.; Kobus, S.; Gertzen, C.G.W.; Hoeppner, A.; Holzscheck, N.; Strunk, C.H.; Huber, H.; Jaeger, K.-E.; Gohlke, H.; Kovacic, F.; et al. A Promiscuous Ancestral Enzyme's Structure Unveils Protein Variable Regions of the Highly Diverse Metallo-β-Lactamase Family. *Commun. Biol.* **2021**, *4*, 132. [CrossRef] [PubMed]
44. Colson, P.; Pinault, L.; Azza, S.; Armstrong, N.; Chabriere, E.; La Scola, B.; Pontarotti, P.; Raoult, D. A Protein of the Metallo-Hydrolase/Oxidoreductase Superfamily with Both Beta-Lactamase and Ribonuclease Activity Is Linked with Translation in Giant Viruses. *Sci. Rep.* **2020**, *10*, 21685. [CrossRef]

45. Park, K.S.; Hong, M.-K.; Jeon, J.W.; Kim, J.H.; Jeon, J.H.; Lee, J.H.; Kim, T.Y.; Karim, A.M.; Malik, S.K.; Kang, L.-W.; et al. The Novel Metallo-β-Lactamase PNGM-1 from a Deep-Sea Sediment Metagenome: Crystallization and X-Ray Crystallographic Analysis. *Acta Crystallogr. Sect. F Struct. Biol. Commun.* **2018**, *74*, 644–649. [CrossRef]
46. Miller, S.Y.; Colquhoun, J.M.; Perl, A.L.; Chamakura, K.R.; Kuty Everett, G.F. Complete Genome of *Bacillus subtilis* Myophage Grass. *Genome Announc.* **2013**, *1*, e00857-13. [CrossRef] [PubMed]
47. Willms, I.M.; Hoppert, M.; Hertel, R. Characterization of *Bacillus subtilis* Viruses vB_BsuM-Goe2 and vB_BsuM-Goe3. *Viruses* **2017**, *9*, 146. [CrossRef]
48. Youle, M.; Pantéa, L. *Thinking Like a Phage: The Genius of the Viruses That Infect Bacteria and Archaea*; Wholon: San Diego, CA, USA, 2017; pp. 1–4.
49. Hobbs, S.J.; Wein, T.; Lu, A.; Morehouse, B.R.; Schnabel, J.; Leavitt, A.; Yirmiya, E.; Sorek, R.; Kranzusch, P.J. Phage Anti-CBASS and Anti-Pycsar Nucleases Subvert Bacterial Immunity. *Nature* **2022**, *605*, 522–526. [CrossRef]
50. Cohen, D.; Melamed, S.; Millman, A.; Shulman, G.; Oppenheimer-Shaanan, Y.; Kacen, A.; Doron, S.; Amitai, G.; Sorek, R. Cyclic GMP–AMP Signalling Protects Bacteria against Viral Infection. *Nature* **2019**, *574*, 691–695. [CrossRef] [PubMed]
51. Tal, N.; Morehouse, B.R.; Millman, A.; Stokar-Avihail, A.; Avraham, C.; Fedorenko, T.; Yirmiya, E.; Herbst, E.; Brandis, A.; Mehlman, T.; et al. Cyclic CMP and Cyclic UMP Mediate Bacterial Immunity against Phages. *Cell* **2021**, *184*, 5728–5739.e16. [CrossRef]
52. Lee, S.Y.; Brem, J.; Pettinati, I.; Claridge, T.D.W.; Gileadi, O.; Schofield, C.J.; McHugh, P.J. Cephalosporins Inhibit Human Metallo β-Lactamase Fold DNA Repair Nucleases SNM1A and SNM1B/Apollo. *Chem. Commun.* **2016**, *52*, 6727–6730. [CrossRef]
53. Lee, J.H.; Takahashi, M.; Jeon, J.H.; Kang, L.-W.; Seki, M.; Park, K.S.; Hong, M.-K.; Park, Y.S.; Kim, T.Y.; Karim, A.M.; et al. Dual Activity of PNGM-1, a Metallo-β-Lactamase and tRNase Z, Pinpoints the Evolutionary Origin of Subclass B3 Metallo-β-Lactamases. *bioRxiv* **2019**, *8*, 575373. [CrossRef]
54. Khan, A.U.; Maryam, L.; Zarrilli, R. Structure, Genetics and Worldwide Spread of New Delhi Metallo-β-Lactamase (NDM): A Threat to Public Health. *BMC Microbiol.* **2017**, *17*, 101. [CrossRef] [PubMed]
55. Malgapo, M.I.P.; Safadi, J.M.; Linder, M.E. Metallo-β-Lactamase Domain-Containing Protein 2 Is S-Palmitoylated and Exhibits Acyl-CoA Hydrolase Activity. *J. Biol. Chem.* **2021**, *296*, 100106. [CrossRef]
56. Katoh, K.; Standley, D.M. MAFFT Multiple Sequence Alignment Software Version 7: Improvements in Performance and Usability. *Mol. Biol. Evol.* **2013**, *30*, 772–780. [CrossRef]
57. Rozewicki, J.; Li, S.; Amada, K.M.; Standley, D.M.; Katoh, K. MAFFT-DASH: Integrated Protein Sequence and Structural Alignment. *Nucleic Acids Res.* **2019**, *47*, W5–W10. [CrossRef] [PubMed]
58. Bottoni, C.; Perilli, M.; Marcoccia, F.; Piccirilli, A.; Pellegrini, C.; Colapietro, M.; Sabatini, A.; Celenza, G.; Kerff, F.; Amicosante, G.; et al. Kinetic Studies on CphA Mutants Reveal the Role of the P158-P172 Loop in Activity versus Carbapenems. *Antimicrob. Agents Chemother.* **2016**, *60*, 3123–3126. [CrossRef]
59. Horsfall, L.E.; Izougarhane, Y.; Lassaux, P.; Selevsek, N.; Liénard, B.M.R.; Poirel, L.; Kupper, M.B.; Hoffmann, K.M.; Frère, J.-M.; Galleni, M.; et al. Broad Antibiotic Resistance Profile of the Subclass B3 Metallo-β-Lactamase GOB-1, a Di-Zinc Enzyme. *FEBS J.* **2011**, *278*, 1252–1263. [CrossRef]
60. Segatore, B.; Massidda, O.; Satta, G.; Setacci, D.; Amicosante, G. High Specificity of cphA-Encoded Metallo-Beta-Lactamase from *Aeromonas hydrophila* AE036 for Carbapenems and Its Contribution to Beta-Lactam Resistance. *Antimicrob. Agents Chemother.* **1993**, *37*, 1324–1328. [CrossRef]
61. Bebrone, C.; Anne, C.; De Vriendt, K.; Devreese, B.; Rossolini, G.M.; Van Beeumen, J.; Frère, J.-M.; Galleni, M. Dramatic Broadening of the Substrate Profile of the *Aeromonas Hydrophila* CphA Metallo-β-Lactamase by Site-Directed Mutagenesis. *J. Biol. Chem.* **2005**, *280*, 28195–28202. [CrossRef]
62. Venkatachalam, K.V.; Huang, W.; LaRocco, M.; Palzkill, T. Characterization of TEM-1 Beta-Lactamase Mutants from Positions 238 to 241 with Increased Catalytic Efficiency for Ceftazidime. *J. Biol. Chem.* **1994**, *269*, 23444–23450. [CrossRef]
63. De Wals, P.-Y.; Doucet, N.; Pelletier, J.N. High Tolerance to Simultaneous Active-Site Mutations in TEM-1 β-Lactamase: Distinct Mutational Paths Provide More Generalized β-Lactam Recognition. *Protein Sci.* **2009**, *18*, 147–160. [CrossRef] [PubMed]
64. Poirel, L.; Héritier, C.; Tolün, V.; Nordmann, P. Emergence of Oxacillinase-Mediated Resistance to Imipenem in *Klebsiella pneumoniae*. *Antimicrob. Agents Chemother.* **2004**, *48*, 15–22. [CrossRef]
65. Robin, F.; Delmas, J.; Machado, E.; Bouchon, B.; Peixe, L.; Bonnet, R. Characterization of the Novel CMT Enzyme TEM-154. *Antimicrob. Agents Chemother.* **2011**, *55*, 1262–1265. [CrossRef]
66. Marcoccia, F.; Leiros, H.-K.S.; Aschi, M.; Amicosante, G.; Perilli, M. Exploring the Role of L209 Residue in the Active Site of NDM-1 a Metallo-β-Lactamase. *PLoS ONE* **2018**, *13*, e0189686. Available online: https://journals.plos.org/plosone/article?id=10.1371/journal.pone.0189686 (accessed on 1 July 2024). [CrossRef]
67. Chiou, J.; Cheng, Q.; Shum, P.T.; Wong, M.H.; Chan, E.W.; Chen, S. Structural and Functional Characterization of OXA-48: Insight into Mechanism and Structural Basis of Substrate Recognition and Specificity. *Int. J. Mol. Sci.* **2021**, *22*, 11480. [CrossRef]
68. Mammeri, H.; Galleni, M.; Nordmann, P. Role of the Ser-287-Asn Replacement in the Hydrolysis Spectrum Extension of AmpC β-Lactamases in *Escherichia coli*. *Antimicrob. Agents Chemother.* **2009**, *53*, 323–326. [CrossRef] [PubMed]

69. Mazzariol, A.; Cornaglia, G.; Nikaido, H. Contributions of the AmpC β-Lactamase and the AcrAB Multidrug Efflux System in Intrinsic Resistance of *Escherichia coli* K-12 to β-Lactams. *Antimicrob. Agents Chemother.* **2000**, *44*, 1387–1390. [CrossRef]
70. Lenfant, F.; Petit, A.; Labia, R.; Maveyraud, L.; Samama, J.-P.; Masson, J.-M. Site-Directed Mutagenesis of β-Lactamase TEM-1. *Eur. J. Biochem.* **1993**, *217*, 939–946. [CrossRef]